Transition to Chaos via Gluing Bifurcations in Optically Excited Nematic Liquid Crystals

G. Demeter and L. Kramer
Physikalisches Institut der Universität Bayreuth, D-95440 Bayreuth, Germany
(Received 1 June 1999; revised manuscript received 13 September 1999)

We study the passage of monochromatic, cw laser light through a cell of homeotropically aligned nematic liquid crystal at a slightly oblique angle, polarized perpendicular to the plane of incidence. Experiments in this geometry have revealed complex, time-dependent dynamics of the director motion. We derive a model for the director dynamics that shows both periodic and chaotic behavior at different light intensities as observed in the experiments. It follows an uncommon route to chaos via gluing bifurcations which has not yet been observed in any real physical system.

PACS numbers: 42.70.Df, 05.45.Ac, 42.65.Sf

Liquid crystals (LCs) are known to produce a great variety of interesting optic phenomena, in particular those associated with the so-called light-induced director reorientation. LCs are optically anisotropic materials, and their local optical properties (the direction of the optical axis) are determined by the orientation of the director. This, on the other hand, is influenced by the electric field of a light wave. Thus an intense light wave can alter the optical properties of the material it propagates through, which leads to a rich variety of nonlinear optical responses of the LC (see Ref. [1]).

An interesting configuration is that of a linearly polarized light wave incident on a cell of a homeotropically aligned nematic at a small angle s_0 with the direction of polarization perpendicular to the plane of incidence [see Fig. 1(a)]. Early experiments have revealed periodic and irregular motions of the director [2,3]. Recently, there has been considerable experimental effort to explore the properties of the irregular regime [4,5]. Observations show that the initial oscillations grow more complex as the intensity of the incident laser beam increases, eventually turning chaotic. While attempts at deriving a model for this complex behavior have begun [6], a proper theory derived from the basic equations which reproduce this chaotic behavior has not yet been published.

In this Letter we report on the derivation of a set of ordinary differential equations (ODEs) for the motion of the director from the fundamental equations for LCs and electromagnetic waves. Computer simulations show that they indeed give rise to complex and chaotic dynamics in good agreement with existing experiments. The model is shown to take a rather distinct route to chaos through a series of gluing bifurcations [7]. To our knowledge, this route to chaos has never been experimentally observed in any real physical system. Therefore this relatively simple system is interesting from the point of view of basic chaos theory.

We start from the basic nematodynamic equations for the director $\vec{n}$ and the velocity field $\vec{v}$, see, e.g., [8]. Since the time scale of the phenomena to be discussed is of the order of seconds, one can neglect inertial terms in the Navier-Stokes equation. We consider solutions that depend only on the z coordinate and then $\vec{v}$ can be eliminated adiabatically. One is left with the director equation $\gamma \dot{n}_i = (\delta_{i,j} - n_i n_j)\delta F/\delta n_j$, where γ is an effective rotational viscosity including the so-called backflow effects, see, e.g., [9]. F is the usual orientational free energy, including the dielectric contribution averaged over the optical frequency oscillations [1]. Assuming homeotropic alignment with strong anchoring at the boundaries, we introduce two angles $\theta(z,t)$ and $\varphi(z,t)$ (see Fig. 1) to describe the director. We assume that these angles are small ($|\theta|, |\varphi| \leq 1$) and write all expressions to third-order accuracy in them.

The electric field $\vec{E}(\vec{r},t)$ is obtained from Maxwell's wave equations with the z-dependent dielectric tensor given by $\epsilon_{ij} = \varepsilon_\perp \delta_{ij} + \varepsilon_a n_i n_j$ (here $\varepsilon_\perp$ is the dielectric permittivity perpendicular to $\vec{n}$ and $\varepsilon_a = \varepsilon_\| - \varepsilon_\perp$ is the dielectric anisotropy). Assuming the incident light to be a monochromatic plane wave, we can apply the formalism of Oldano for electromagnetic wave propagation in anisotropic stratified media [10]. With its help, it is possible to write a set of ODEs for the z dependence of the field components and formally solve it by using perturbation theory to third order in the angles θ, φ. We then substitute these expressions (which contain multiple integrals of the angles with respect to z in a complicated way) into the director equations to get a set of equations

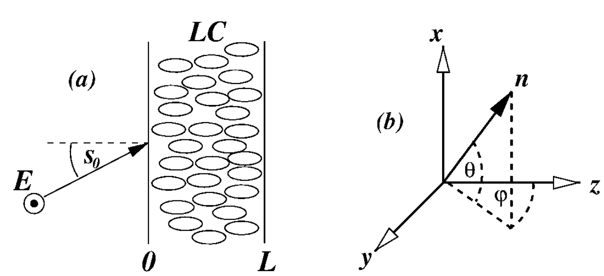

FIG. 1. (a) Geometry of the setup: a slightly oblique ordinary wave incident upon a cell of nematic LC with homeotropic orientation. (b) Definition of the angles describing the orientation of the director.

 0031-9007/99/83(23)/4744(4)$15.00

of motion for the angles. These are still partial differential equations in z and t, but we can now expand in terms of sine functions $\varphi(z,t) = \sum_n A_n(t)\sin(n\pi z/L)$, $\theta(z,t) = \sum_n B_n(t)\sin(n\pi z/L)$ (L is the thickness of the cell) which satisfy the boundary conditions. We project the original system of equations on these modes to get a set of coupled, first-order, nonlinear ODEs for the amplitudes $A_n(t), B_n(t)$. This set must be truncated yielding a finite vector of variables $(A_1, \ldots, A_n, B_1, \ldots, B_m)$. The equations can be simplified by keeping only the terms up to third order in the amplitudes. Their general form is

$$\begin{aligned} \tau \dot{A}_i &= -i^2 A_i + \sum_j L^A_{ij} A_j + \sum_{j,k} P^A_{ijk} A_j B_k \\ &\quad + \sum_{\substack{j,k,l \\ k\le l}} Q^A_{ijkl} A_j B_k B_l + \sum_{j\le k\le l} R^A_{ijkl} A_j A_k A_l \,, \\ \tau \dot{B}_i &= -i^2 B_i + \sum_{j\le k} P^B_{ijk} A_j A_k + \sum_{\substack{j,k,l \\ k\le l}} Q^B_{ijkl} B_j A_k A_l \\ &\quad + \sum_{j\le k\le l} R^B_{ijkl} B_j B_k B_l. \end{aligned} \tag{1}$$

The linear coefficients L^A and the nonlinear terms P^A, Q^A, R^A, P^B, Q^B, and R^B are functions of $s = s_0/\sqrt{\varepsilon_\perp}$ (the angle of refraction of an ordinary wave in the cell), $\varepsilon_a' = \varepsilon_a/\varepsilon_\perp$, the ratios of the Frank constants K_1/K_3, K_2/K_3, the intensity parameter ρ defined as

$$\rho = \frac{I}{I_F}, \qquad I_F = \frac{\pi^2}{L^2}\,\frac{c(\varepsilon_\perp + \varepsilon_a)K_3}{\varepsilon_a\sqrt{\varepsilon_\perp}} \tag{2}$$

(I is the laser intensity, I_F is the threshold intensity of the light-induced Fréedericksz transition (LIFT) for perpendicular incidence), and the parameter κ, where

$$\kappa = \frac{L}{\pi}\,\frac{s_0^2\varepsilon_a k_0}{2\sqrt{\varepsilon_\perp}(\varepsilon_\perp + \varepsilon_a)} \tag{3}$$

(k_0 is the wave number of the incident light in vacuum). κ is (to a very good approximation) the phase shift between an ordinary and an extraordinary wave (the latter is polarized in the plane of incidence and the former is perpendicular to this plane) at $z = L$ for the undisturbed homeotropic alignment of the LC. The characteristic time τ is given by $\tau = \gamma L^2/\pi^2 K_3$. ρ is the control parameter in the problem. Because of the inversion symmetry with respect to the x, z plane the equations are invariant under the transformation $S{:}\{A_i, B_k\} \to \{-A_i, B_k\}$.

Clearly, in the linear destabilization of the basic state, only the modes A_i are active. For normal incidence (then $\kappa = 0$), one has $L_{ij} = \rho\delta_{ij}$, so that only A_1 is activated at the Fréedericksz transition occurring at $\rho = 1$. For small angles of incidence it suffices to keep A_1 and A_2 because the linear damping of the modes due to elastic stress grows proportional to i^2, and A_3 and higher modes are only weakly coupled to the first two. The resulting linear stability analysis [6] shows destabilization in a stationary pitchfork bifurcation for values of the phase shift below some κ_c, and against a Hopf bifurcation above that. Figure 2 shows these results in the ρ, κ plane.

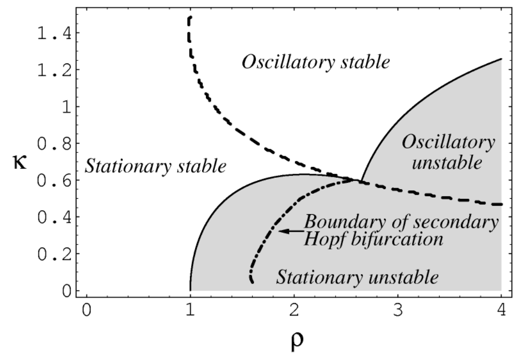

FIG. 2. Stability diagram of the homogeneous state. In the region of instability (grey) the complex growth rate of perturbations has a positive real part. To the right of the dashed line the maximum growth rate has a nonzero imaginary part. The basic state is unstable against a stationary bifurcation for $\kappa \le 0.6$ and against a Hopf bifurcation in the region above that. The dashed-dotted line marks the secondary Hopf bifurcation of the stationary reoriented state as calculated numerically from the nonlinear model.

The complicated expressions for the nonlinear terms can be simplified considerably by using the inequalities $s \ll 1$ and $\kappa^2 \ll 1$. The latter does not follow simply from the former because $Lk_0 \gg 1$. However, by using values for the parameters that correspond to the experiments [12], we get $\kappa^2 \approx 0.06$. We display here in the small κ limit the linear coefficients, $L^A_{ii} = \rho + \kappa^2\rho\frac{1+2(-1)^i}{i^2}$ and $L^A_{ij} = 2\kappa^2\rho\frac{(-1)^j}{i\cdot j}$, $j \ne i$. The rest will be published in a forthcoming paper together with a detailed derivation.

For the nonlinear analysis we supplement the modes A_1 and A_2 by B_1. At least these modes are needed to obtain the observed scenario. On the other hand, they should suffice for not too large ρ because of the strong linear damping of the higher modes. In fact it turns out that the behavior of this minimal model already describes very well the observations in the experiments.

While the equations of even this simplest three-variable model cannot be solved analytically, one can easily explore the model's behavior by numerically solving the equations with different parameters. Here we present a short summary of the behavior as ρ is increased with the rest of the parameters corresponding to the setup used in the experiments [4,5] (see Ref. [12]).

The basic state ($A_1 = A_2 = B_1 = 0$) loses stability at $\rho_c \approx 1.065$ and stationary reorientation takes place (LIFT). The symmetry S is broken spontaneously. In the region of interest above ρ_c the basic state is a saddle point with three real eigenvalues $\lambda_3 < \lambda_2 < 0 < \lambda_1$, and one has two symmetry degenerate off-origin fixed points. Not too far above ρ_c the amplitude A_1 dominates which corresponds to a simple sinusoidal reorientation in the y direction. At higher intensities, the nonlinear interaction between the modes becomes important leading to the growth of A_2 and B_1.

The stationary reoriented state becomes unstable in a Hopf bifurcation at $\rho_0 \approx 1.71$ and two simple limit cycles appear in phase space which are mutual images under S [see Fig. 3(a)]. The period of these limit cycles is $T \approx 13.5$ s at $\rho = 1.72$ just above the bifurcation and grows with increasing ρ. As the light intensity increases, the radius of the limit cycles grows, and at $\rho_1 \approx 1.808\,75$ the two limit cycles merge in a gluing bifurcation at the origin. At ρ_1 the limit cycles are homoclinic trajectories which leave the origin along the λ_1 direction and return along the λ_2 direction. Figure 3(b) shows this situation. Slightly above ρ_1 one has a single double-length limit cycle [Fig. 3(c)] which is symmetric under S. This is not a period-doubling bifurcation, however, as the homoclinic trajectories at ρ_1 have an infinite period.

At a certain intensity, $\rho_1' > \rho_1$, the symmetric limit cycle loses stability and two asymmetric limit cycles are born that are mutual images under S [Fig. 4(a)]. These merge in a second gluing bifurcation at $\rho_2 \approx 1.9474$, where the limit cycles are again homoclinic trajectories with an infinite period. The symmetric quadruple-length limit cycle that is stable just above ρ_2 is shown in Fig. 4(b). This sequence of splitting and remerging of the limit cycle continues and the set of values ρ_i converge to a value $\rho_\infty \approx 1.98$. Beyond this point the motion is chaotic. The system exhibits typical signatures of low-dimensional deterministic chaos such as great sensitivity to initial conditions and a positive Lyapunov exponent. The frequency spectrum of the mode amplitudes also shows this transition to chaos by changing from a line spectrum (where all lines are integer multiples of the same fundamental frequency) to a continuous spectrum. Figure 5 shows motion along the Lorenz-like strange attractor at $\rho = 2.2$. The largest Lyapunov exponent at this intensity is $\lambda_L = 0.0885\ \mathrm{s}^{-1}$.

The important property of our equations that allows this route to chaos is the invariance under S and the fact that $-\lambda_2 > \lambda_1$ up to about $\rho \approx 2.13$. This latter property allows the homoclinic trajectories to be stable [7]. The inclusion of more modes and/or higher-order terms in our model would preserve these properties (in the small κ^2 limit). The famous Lorenz system has identical symmetry properties but has $-\lambda_2 < \lambda_1$ and thus follows a different route to chaos.

At about $\rho = 2.5$ the Lorenz-like symmetric attractor gives way to two asymmetric attracting sets, again mutual images under S. They are of the form of a Möbius strip and the scenario is similar to that occurring in the Shimizu-Morioka model [13]. As the intensity is increased, the system returns to simple periodic behavior via an inverse period-doubling cascade.

A qualitative comparison of our simulations and the experimental observation shows that our model exhibits

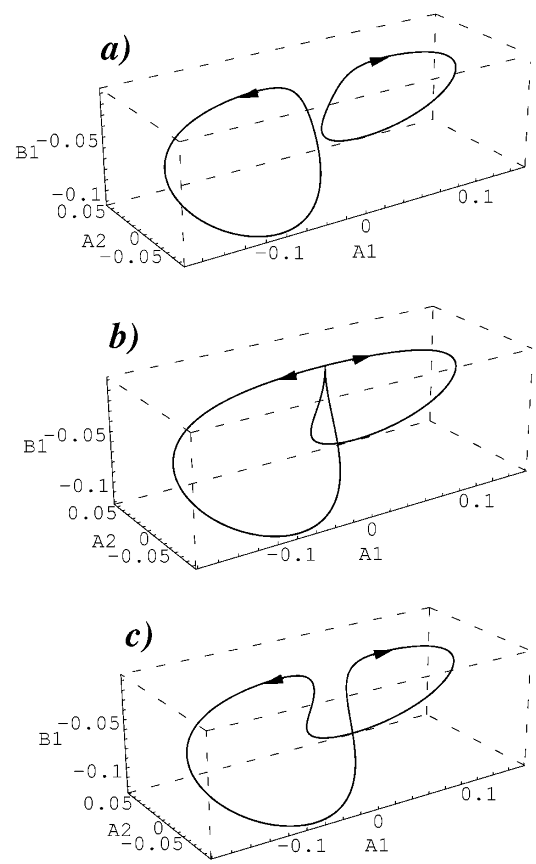

FIG. 3. (a) Simple limit cycles in three-dimensional phase space spanned by A_1, A_2, and B_1 at $\rho = 1.78$. (b) The limit cycle at $\rho = 1.808\,75$ at the first gluing bifurcation where it is composed of two homoclinic trajectories with infinite periods. (c) The double-length limit cycle at $\rho = 1.85$.

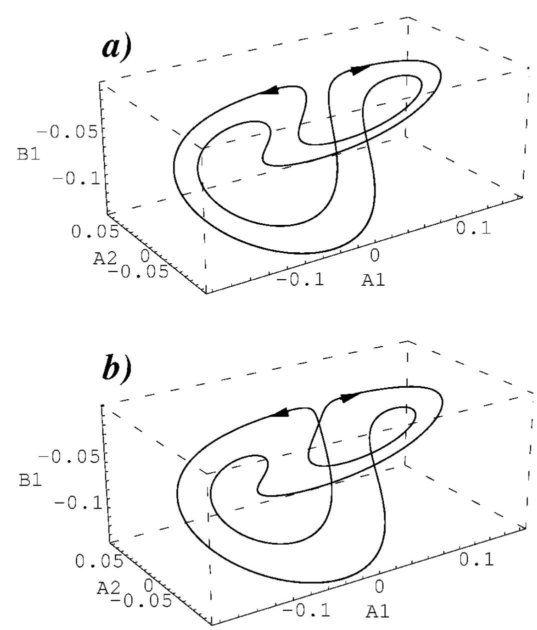

FIG. 4. (a) $\rho = 1.94$, two asymmetric limit cycles which are mutual images under S. (b) $\rho = 1.96$, symmetric limit cycle born in the second gluing bifurcation.

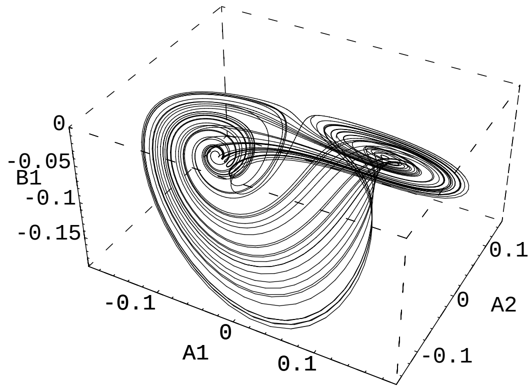

FIG. 5. Motion on the Lorenz-like strange attractor at $\rho = 2.2$. The largest Lyapunov exponent of the attractor is $\lambda_L = 0.0885\ \mathrm{s}^{-1}$.

periodic oscillations, transition to chaos and a return to periodic behavior, just as observed in some of the experiments [4]. At still higher intensities, chaotic behavior was observed again, but our simulations do not display this property, so refining of the model is eventually needed. A quantitative comparison is hampered by the fact that the precise behavior of the model depends sensitively on the values of the parameters and we have limited information on the precise experimental values [12]. Furthermore, the transition to chaos was only qualitatively described in the experimental papers [4,5]. The threshold intensity of the onset of periodic behavior ($\rho = 1.71$) is, however, quite near to the experimental values. The system was observed to already be in the oscillatory regime at $\rho \approx 1.86$ in [4] with the period of the oscillations being $T \approx 12.5$ s. Our model exhibits sizable oscillations at $\rho = 1.73$ with period $T \approx 14$ s. The predicted increase of the period of the oscillations with ρ in the first oscillatory regime (before the first gluing bifurcation) is also in agreement with observations. The largest Lyapunov exponent of the attractor in the chaotic regime found in the experiments ($0.1 \pm 0.015\ \mathrm{s}^{-1}$) is consistent with that found in our simulations ($0.0885\ \mathrm{s}^{-1}$ at $\rho = 2.2$). We finally mention that the general features of the model are quite robust, as can be seen, e.g., from the κ dependence of the secondary Hopf bifurcation shown in Fig. 2 (dashed-dotted line).

In conclusion, the model we have constructed describes periodic and chaotic director oscillations in nematics excited by a slightly oblique incident laser wave. There is good qualitative and fair quantitative agreement with existing experiments in the regions of lower intensity. The solutions obtained are consistent with the initial assumption of small angles, as none of the amplitudes ever surpasses 0.2. To our knowledge, this is the first theory for these phenomena that have been observed in experiments for nearly two decades. Furthermore, our model suggests that the route this system follows to chaos is one which has, to our knowledge, not been observed in any experiment before. This makes a further study of the system interesting not only from the point of view of LC nonlinear optics but from that of basic chaos theory. Among the predictions that could be tested in further experiments we mention the predicted drastic increase of the period in the vicinity of the gluing bifurcations and the interesting codimension-2 point, where the primary Hopf bifurcation joins with the secondary one.

We wish to thank P. Coullet and M. A. Zaks for helpful discussions. The hospitality of the Max Planck Institute for the Physics of Complex Systems in Dresden, Germany, where part of this research was carried out, is gratefully acknowledged.

[1] N. V. Tabiryan, A. V. Sukhov, and B. Ya. Zel'dovich, Mol. Cryst. Liq. Cryst. **136**, 1–140 (1985); F. Simoni, *Nonlinear Optical Properties of Liquid Crystals* (World Scientific, Singapore, 1997).

[2] B. Ya. Zel'dovich *et al.*, JETP Lett. **37**, 677 (1983).

[3] A. S. Zolot'ko *et al.*, Sov. Phys. JETP **60**, 488 (1984); V. F. Kitaeva *et al.*, Sov. Phys. JETP **62**, 520 (1985).

[4] G. Cipparrone *et al.*, Phys. Rev. E **47**, 3741 (1993).

[5] V. Carbone *et al.*, Mol. Cryst. Liq. Cryst. **251**, 167 (1994); V. Carbone *et al.*, Phys. Rev. E **54**, 6948 (1996); C. Versace *et al.*, Mol. Cryst. Liq. Cryst. **290**, 267 (1996).

[6] N. V. Tabiryan *et al.*, Opt. Commun. **154**, 70 (1998).

[7] A. Arneodo, P. Coullet, and C. Tresser, Phys. Lett. **81A**, 197 (1981); Y. Kuramoto and S. Koga, Phys. Lett. **92A**, 1 (1982); D. V. Lyubimov and M. A. Zaks, Physica (Amsterdam) **9D**, 52 (1983).

[8] H. Pleiner and H. R. Brand, in *Pattern Formation in Liquid Crystals*, edited by A. Buka and L. Kramer (Springer, New York, 1996).

[9] E. Guyon, R. Meyer, and J. Salan, Mol. Cryst. Liq. Cryst. **54**, 261 (1979).

[10] C. Oldano, Phys. Rev. A **40**, 6014 (1989).

[11] G. Cipparrone *et al.*, Mol. Cryst. Liq. Cryst. **266**, 263 (1995).

[12] The parameters that correspond to the experimental setup [4,5] are $L = 50\ \mu$m, $s_0 = 0.122$, and $\lambda = 514$ nm. For the parameters of the chemical E7 used we took, for the ratios of the Frank constants, $K_1/K_3 = 2/3$ (British Drug House data sheet) and $K_2/K_3 = 1/2$ (our estimate). The ratio K_3/γ was taken to be $10^{-6}\ \mathrm{cm}^2/\mathrm{s}$ from a direct measurement in the same geometry [11]. This value should already include the backflow effects. For the dielectric constants at optical frequency we took $\varepsilon_\perp = 2.25$ and $\varepsilon_a = 0.76$ from [6].

[13] A. L. Shil'nikov, Physica (Amsterdam) **62D**, 338 (1993).